Robustness and Reliability of Synergy-Based Myocontrol of a Multiple Degree of Freedom Robotic Arm

Francesca Lunardini, Claudia Casellato, *Member, IEEE*, Andrea d'Avella, *Member, IEEE*, Terence D. Sanger, *Member, IEEE*, and Alessandra Pedrocchi, *Member, IEEE*

***Abstract*—In this study, we test the feasibility of the synergy-based approach for application in the realistic and clinically oriented framework of multi-degree of freedom (DOF) robotic control. We developed and tested online ten able-bodied subjects in a semi-supervised method to achieve simultaneous, continuous control of two DOFs of a robotic arm, using muscle synergies extracted from upper limb muscles while performing flexion-extension movements of the elbow and shoulder joints in the horizontal plane. To validate the efficacy of the synergy-based approach in extracting reliable control signals, compared to the simple muscle-pair method typically used in commercial applications, we evaluated the repeatability of the algorithm over days, the effect of the arm dynamics on the control performance, and the robustness of the control scheme to the presence of co-contraction between pairs of antagonist muscles. Results showed that, without the need for a daily calibration, all subjects were able to intuitively and easily control the synergy-based myoelectric interface in different scenarios, using both dynamic and isometric muscle contractions. The proposed control scheme was shown to be robust to co-contraction between antagonist muscles, providing better performance compared to the traditional muscle-pair approach. The current study is a first step toward user-friendly application of synergy-based myocontrol of assistive robotic devices.**

***Index Terms*—Assistive robotics, muscle synergies, myoelectric control, myoelectric signal processing.**

I. Introduction

A MYOELECTRIC control system is one in which operation of the output apparatus is controlled by the surface electromyogram (EMG) recorded during the contraction of one or more muscles [1]. The main advantage of myoelectric control is due to the ability of the EMG signal to noninvasively convey information about the human motor intent [2].

In recent decades, intensive effort has been devoted to the development of intuitive control schemes able to provide user-friendly controllers. Starting from the early 1960s, a number of studies addressed this challenge using pattern recognition techniques. This approach decodes muscle activity into intuitive outputs by training a model on a dataset that associates EMG signals with desired motor outputs [3], [4]. These algorithms showed high classification accuracy of joint kinematics in offline performance [5]. However, EMG signals are classified in a limited number of patterns, thus obtaining a discrete approximation of the continuous parameter space. As a consequence, the controller is sequential, since only one pattern at a time can be selected. In addition, proportional control is challenging to achieve, since proportionality in the commands undermines the classification accuracy [6]. Therefore, the unnatural discrete non-proportional control scheme achieved by the pattern classification approach results in the lack of a successful clinical application of this technique. Nowadays, robust continuous proportional and simultaneous myoelectric control, in which multiple degrees of freedom (DOFs) can be controlled at the same time via EMG inputs, is a necessary requirement for commercial applications in robotic control, prostheses, and orthoses [7]–[10]. A simple control strategy is represented by two independent muscles controlling each single DOF [1], [11]. Due to its simplicity, this approach is generally adopted by available prostheses today [12], [13]. However, these systems are inherently limited since this strategy neglects information from multiple muscles acting on each DOF and simultaneous control of different DOFs can be achieved only if each muscle is involved in the activation of only one DOF (i.e., mono-articular muscles). In addition, as a consequence of recording activity from only a pair of independent muscles for each DOF, this approach is less robust to the noise that may affect the stochastic EMG signal [14]. To overcome the above-mentioned limits, some studies proposed myoelectric controllers based on regression methods [15], [16] which provide estimation of joint kinematics or kinetics, based on the subject's multi-site muscle activity. In this framework, some studies [17], [18] tested an approach based on the synergy model, a motor control model which assumes that low-dimensional and high-level neural commands are translated into high-dimensional and low-level patterns of muscle activity [19], [20]. Regardless of their physiological origin, time-invariant muscle synergies, extracted from

Manuscript received April 09, 2015; revised July 13, 2015; accepted September 07, 2015. Date of publication September 30, 2015; date of current version September 05, 2016. *Corresponding author: F. Lunardini* (e-mail: francesca.lunardini@polimi.it).

F. Lunardini, C. Casellato, and A. Pedrocchi are with the Department of Electronics, Information and Bioengineering, NearLab, Politecnico di Milano, 20133 Milano, Italy (e-mail: francesca.lunardini@polimi.it; claudia.casellato@polimi.it; alessandra.pedrocchi@polimi.it).

A. d'Avella is with the Department of Neuromotor Physiology, Foundation Santa Lucia, 00142 Rome, Italy, and the Department of Biomedical and Dental Sciences and Morphofunctional Imaging, University of Messina, 98122 Messina, Italy (e-mail: a.davella@hsantalucia.it).

T. D. Sanger is with the Department of Biomedical Engineering, Neurology, and Biokinesiology and Physical Therapy, University of Southern California, Los Angeles, CA USA (e-mail: terry@sangerlab.net).

Color versions of one or more of the figures in this paper are available online at http://ieeexplore.ieee.org.

Digital Object Identifier 10.1109/TNSRE.2015.2483375

multiple EMG channels while performing a number of different tasks, represent underlying muscle coordination principles [21], [22], making it possible to describe a variety of EMG patterns as a combination of these fixed muscle synergies. Berger and colleagues [18] tested a synergy-to-force mapping to validate muscle synergies as a neural control strategy in cursor control tasks. However, the robustness of control strategies based on regression methods strongly depends on the training dataset, which should be representative of a wide set of possible movements. To do so, the algorithm may require a long and intensive training phase, which, in addition, may not be possible in certain groups of patients, since it requires the availability of both EMG and kinematic signals.

A solution to the supervision problem has been proposed in recent studies that used the synergy model to achieve continuous proportional and simultaneous control of multiple DOFs without the need for a time-demanding training phase [23]–[25]. In particular, Jiang and colleagues [24] achieved simultaneous continuous control of two DOFs with a semi-supervised approach that did not require a training session, but only a short initial calibration with information about which DOF was active. This piece of information was needed to associate each single muscle synergy, extracted using a modified version of the Nonnegative Matrix Factorization (NMF) algorithm (DOF-wise NMF) [26], to the related DOF. The efficacy of this control strategy has been shown in able-bodied subjects [27], as well as in amputees [28], both during offline tests and online validations involving two-dimensional cursor control on a computer monitor. However, the efficacy of these control schemes needs to expand from the traditional cursor control and demonstrate robustness in more realistic applications, such as robotic control [29]. Differences between a simple cursor control and multi-DOF robot control include mechanical constraints and dynamics of the robotic device, and it is reasonable to expect such differences to influence the controller performance.

For the first time, this study tests the synergy-based approach in the more realistic and clinically oriented framework of multi-DOF robotic control. To do so, we developed and tested online, on ten able-bodied subjects, a semi-supervised method to achieve simultaneous, continuous control of two DOFs of a robotic arm that reproduces the user's movement (or intention of movement), using muscle synergies extracted from upper limb muscles while performing flexion-extension movements of the elbow and shoulder joints in the horizontal plane. To test the effect of the dynamics of arm on the control scheme, robotic myocontrol was achieved using EMG signals recorded during both isometric contractions and unconstrained movements executed at different speeds. The experiments were run over multiple days to evaluate the repeatability of the synergy-based algorithm. Our goal, here, was to validate the feasibility and the efficacy of the synergy-based approach for multi-DOF robotic control compared to the simple muscle-pair method typically used in commercial applications. The current study is a first step toward application of synergy-based myocontrol as control strategy for functional or rehabilitative robotic devices.

II. Methods

The study consisted of two protocols. For the first protocol (Dynamic Protocol), muscle synergies and control signals were computed from EMG activity of upper-limb muscles recorded during unconstrained flexion-extension movements of the elbow (DOF 1) and the shoulder (DOF 2) joints in the horizontal plane. In the second protocol (Isometric Protocol), muscle synergies and control signals were extracted from isometric contractions mimicking flexion-extension movements of the two joints in the horizontal plane. The reason to test the Isometric Protocol was that isometric force may be useful for those patients whose irregularities of muscle activity are exacerbated by the dynamics of limb control, as for patients with disorders of the control of muscles.

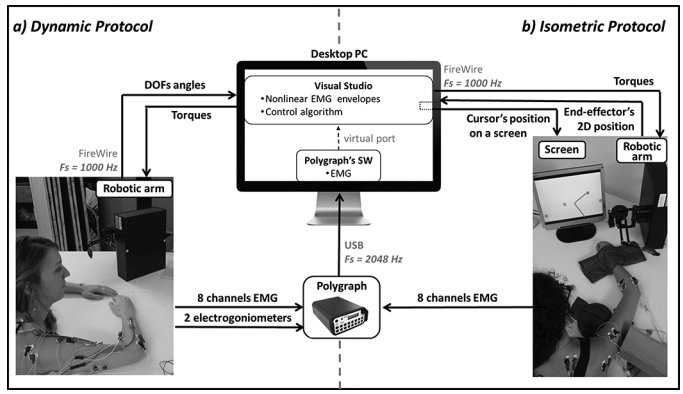

Fig. 1. Experimental setup. A polygraph is used to record, with a sampling frequency of 2048 Hz, the EMG activity from eight upper-limb muscles. The real-time EMG signals are passed to a Desktop PC, where a dedicated software high-pass filters the data before sending them to the C++ control algorithm. The C++ controller processes the data to generate the torque commands actuating the robot's DOFs, with a frequency of 1000 Hz, in order to reproduce the ongoing subject's motion (or intention of motion). Panel a: Dynamic Protocol. The polygraph records the subject's flexion-extension angles elbow and shoulder joints by means of two electrogoniometers. The controller reads the subjects' and the robot's angles, which are stored for postprocessing analyses. Panel b: Isometric Protocol. The controller reads the 2-D position of the robot's end-effector and displays it on a computer screen. In this figure, for clarity purposes, the robot is placed on the table to show the entire apparatus. During the experiments, however, the robot was placed on a side lower table, so that the user could not see the robot's movement.

A. Subjects

Eight healthy subjects (24 to 33 years old) participated in the study. None of the subjects participated in any myoelectric control study prior to the current experiment. All subjects read and signed informed consent. The study was performed in accordance with the Declaration of Helsinki.

B. Experimental Setup

The experimental setup is shown in Fig. 1. Surface EMG signals were acquired using a commercial 32-channel polygraph (PortiTM, Twente Medical System International, The Netherlands) at a sampling rate of 2048 Hz. Surface electrodes were placed in bipolar configuration, with an inter-electrode distance of 10 mm, on the belly of eight upper-limb muscles that are known to contribute to elbow and shoulder movements: Brachioradialis (BRACH), Anconeus (ANC), Biceps Brachii (BIC), Triceps Brachii (TRIC), Anterior Deltoid (AD), Lateral Deltoid (LD), Posterior Deltoid (PD), and Supraspinatus (SS). Prior to electrode placement, the skin over the muscles and the surface of the sensors were wiped with isopropyl alcohol

pads to reduce electrical impedance at the skin electrode interface. The target muscles were mostly found by palpation and anatomical landmarks. EMG signals, high-pass filtered at 5 Hz, were passed, through a virtual port, to a custom C++ program. Nonlinear envelopes of the EMG signals were extracted by applying a nonlinear recursive filter based on Bayesian estimation which produces a smooth output that estimates the driving force underlying the EMG signal with low latency [30], thus guaranteeing online control. In addition, previous studies [29] showed that the use of the nonlinear Bayesian filtering in myoelectric control applications led to more accurate control performance, compared to the use of the traditional linear envelope. The algorithm computed online the torque signals to drive two DOFs of a robotic arm, the Phantom® Premium 1.0 (SensAble™), which is a 3-DOF haptic device. For the purpose of our study, we fixed the first DOF, while the second and the third DOFs of the robot were arranged to mimic flexion-extension movements in the horizontal plane of the shoulder (DOF 2) and the elbow (DOF 1) joints, respectively. The robot's encoders of the two DOFs and the robot's end-effector were recorded with a frequency of 1000 Hz. In the Dynamic Protocol (Fig. 1, panel a), two electrogoniometers (Goniometer Biometrics SG150, 1D, flexible part 115–170 mm, Biometrics Ltd, U.K.), placed on the shoulder and the elbow respectively, were connected to the polygraph to record the subject's joint angles. For the Isometric Protocol (Fig. 1, panel b), a computer screen was positioned in front of the subject, displaying three circular targets and a cursor that tracked online the 2-D position of the robot's end-effector. The diameter of each target was 35 density-independent units (pt), while the entire screen was 505 $\times$ 400 pt.

C. Experimental Protocols

During the experiment, the subject was seated at a table with the dominant arm placed on it. The height of the chair was adjusted so that the weight of the arm and the forearm was supported to avoid any anti-gravitary muscle activity (Fig. 1). During the Dynamic Protocol, friction-reducing sheets were placed between the subject's limb and the table surface. During the Isometric Protocol, heavy weights were placed along both sides of the arm and the forearm to avoid flexion-extension movements, thus ensuring isometric contractions. Both protocols consisted of three phases. The first step was a calibration phase, aimed at recording data to extract offline subject-specific muscle synergies. The calibration was followed by a synergy-based control phase, during which the subject achieved online simultaneous control of the robot's DOFs. A third control phase was designed to implement the traditional muscle-pair approach. Each protocol was executed over two days (Day 1 and Day 2): the calibration phase took place only on Day 1, while online control was repeated on Day 1 and Day 2, using the synergies extracted from the calibration phase data of Day 1. The details of the two protocols and their respective phases are presented as follows.

1) Dynamic Protocol—Calibration Phase:

The subject was instructed to perform a predefined sequence of single-DOF movements (Fig. 2). For the elbow (DOF 1), a sequence of three flexion/extension movements (from 60° to 160°, and back) was executed with the shoulder fixed at 90°, 135°, and 180°. Single-DOF movements for the shoulder (DOF 2) were performed in a similar way: three flexion/extension movements (from 180° to 90° and back) were performed with the elbow fixed at 60°, 105°, and 160°. The EMG signals acquired during this phase were recorded and factorized by applying a DOF-wise NMF to extract the muscle synergy matrix S used for the online control phase, as reported in Section II-D.

Online Synergy-Based Control Phase: In this phase (Fig. 2), the subject was instructed to perform simultaneous flexion-extension movements of the two DOFs. Each participant achieved two types of double-DOFs movements: in the first type, DOF 1 and DOF 2 were first extended and then flexed simultaneously; in the second type, the two DOFs were articulated in opposite directions (i.e., when DOF 1 was flexed, DOF 2 was extended, and vice versa). Each participant performed two sequences per each type, one slower and one faster, for a grand total of four sequences. During online control, to prevent corrective movements to alter the natural flow of the ongoing motion, the user was not allowed to look at the robot.

Offline Muscle-Pair Control Phase: To assess the effectiveness of our approach compared with the traditional muscle-pair method, we performed offline simulations of robot control based on the muscle-pair approach using the same EMG activity recorded during the online synergy-based control phase. Additional details are presented in Section II-E.

2) Isometric Protocol—Calibration Phase:

The subject was instructed to perform predefined sequences of isometric contractions of the two DOFs separately, mimicking the sequences of movements executed during the calibration phase of the Dynamic Protocol. The subject was encouraged to perform isometric contractions of one DOF at a time, trying not to involve the other DOF. For DOF 1, the elbow was positioned at 105° of flexion and the shoulder at 90°, 135°, and 180°. For each configuration of the shoulder, the subject was instructed to perform three series of isometric contractions, mimicking flexion-extension movements. In a similar way, for DOF 2, the subject was asked to perform three series of flexion-extension movements of the shoulder, fixed at 105° of flexion, with the elbow at 90°, 135°, and 180° (Fig. 2). The EMG signals acquired during this phase were recorded and factorized by applying a DOF-wise NMF to extract the S matrix.

Online Synergy-Based Control Phase: In this phase, the participant was seated in front of a monitor displaying three targets and a cursor that tracked online the 2-D position of the robot's end-effector. The three targets were placed at predefined angular positions of the two DOFs. In particular, Target 1 was hit by the robot's end-effector when DOF 1 and DOF 2 were completely extended. Target 2 required DOF 1 to be completely flexed and DOF 2 to be half-way extended. Finally, to hit Target 3, the robot's DOF 1 and DOF 2 had to be halfway extended and halfway flexed, respectively. The subject was instructed to reach each target as fast as possible and to pause with the cursor within the target for at least 2 seconds (threshold time), for the target to be considered hit. The task was accomplished when the subject reached all three targets, regardless from the order, within a 45 seconds time interval. Otherwise, the task was treated as a failure. Each subject performed three trials.

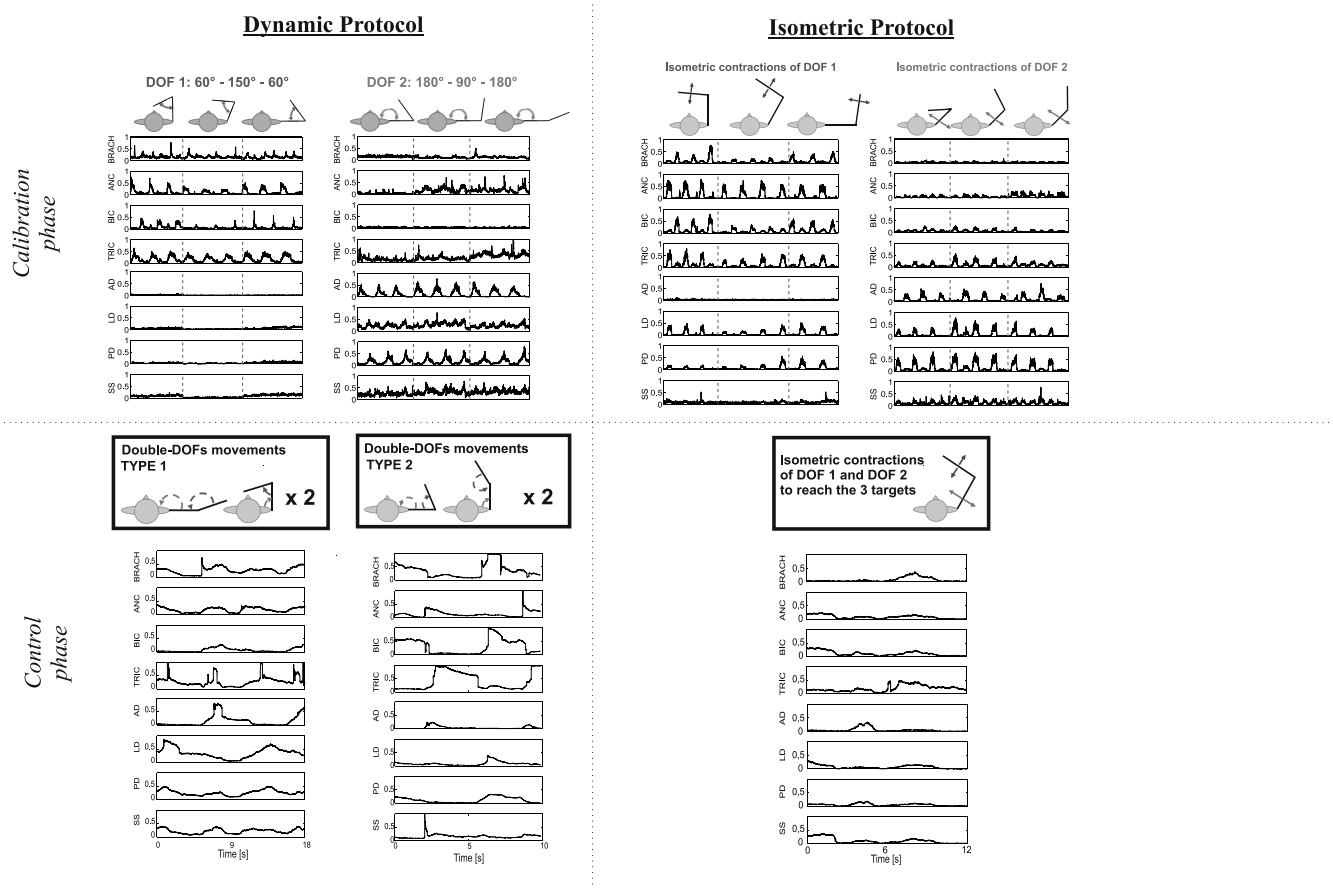

Fig. 2. Experimental protocol. Figure shows the sequences of movements and isometric contractions performed by each subject, together with the envelopes of the recorded EMG activity [Brachioradialis (BRACH), Anconeus (ANC), Biceps Brachii (BIC), Triceps Brachii (TRIC), Anterior Deltoid (AD), Lateral Deltoid (LD), Posterior Deltoid (PD), and Supraspinatus (SS)]. Calibration phase (upper panel) and Control phase (lower panel) are presented for both the Dynamic (left panel) and the Isometric (right panel) Protocols.

Online Muscle-Pair Control Phase: The task was identical to the one described for the synergy-based isometric control, with the only difference being that the robot's DOFs were driven using the muscle-pair approach (see Section II-E for details). As for the synergy approach, each subject repeated the experiment three times.

The order of the two online control phases in the Isometric Protocol was randomized for each subject to avoid any effect of learning in the performance. The subject was blind to which algorithm was used. Before recording, the user was given a training period of three trials.

D. Offline Calibration Data Analysis

Offline calibration data analysis was executed with Matlab R2011b (Mathworks, Natick, MA USA).

The EMG signals acquired during the calibration phases were recorded and factorized by applying a DOF-wise NMF to extract the subject-specific muscle synergy matrix S (Fig. 3). The muscle synergy model [31] assumes that movements are executed by translating low dimensional task-level commands into higher dimensional muscle activation patterns [19]. Based on this theory, matrix factorization algorithms, such as NMF, are commonly used to estimate N-dimensional neural activation signals (A) from M-dimensional muscle signals (X), with N < M. In particular, the activation of the mth muscle, $x_m(t)$, can be modeled as

$$x_{m(t)} = \sum_{n=1}^{N} s_{mn} \cdot a_n\,(t) \tag{1}$$

where s_{mn} is the gain by which the nth activation coefficient, a_n, is transferred to the mth muscle. In matrix form, (1) can be written as

$$X\,(t) = S \cdot A\,(t) \tag{2}$$

where each column of the synergy matrix S represents a muscle synergy. A modified version of the NMF has been proposed for the application of myoelectric control [22]. This DOF-wise NMF models each DOF as driven by two activation signals, one for each direction of articulation of the DOF. Therefore, by applying the NMF algorithm to the single-DOF EMG signals recorded during the calibration phase, it is possible to extract two synergies for each DOF separately and to associate each synergy to Positive ("E") or Negative ("F") directions of that specific DOF. By applying the DOF-wise algorithm to DOF 1

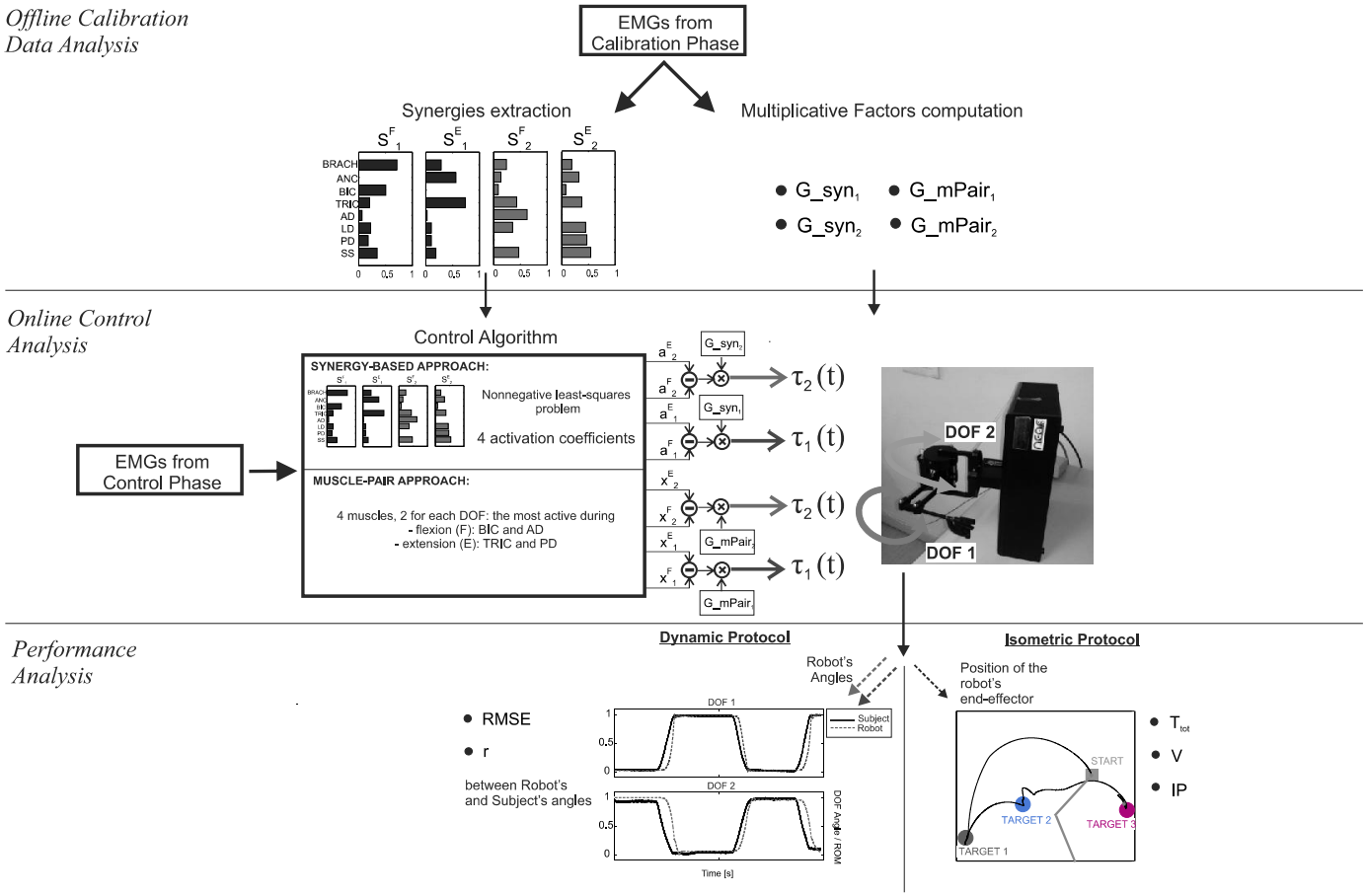

Fig. 3. Analyses. Upper panel: Offline Calibration Data Analysis. Subject's EMG signals recorded during the Calibration Phase are factorized to extract the muscle synergy matrix S and the multiplicative factors $[G\_syn_1, G\_syn_2, G\_m\mathrm{Pair}_1, G\_m\mathrm{Pair}_2]$ used for the online control phase. Middle panel: Online Control Analysis. Synergy-based approach: at each time instant, four activation coefficients $[\mathrm{a}_1^F, \mathrm{a}_1^E, \mathrm{a}_2^F, \mathrm{a}_2^E]$ are estimated online, given the subject's EMGs and S, by solving a nonnegative least squares problem. The activation coefficients are combined to produce the torque commands sent to the robot's actuators. Muscle-pair approach: the activity of the four muscles most involved in each of the two directions of articulation of the 2 DOFs $[\mathrm{x}_1^F, \mathrm{x}_1^E, \mathrm{x}_2^F, \mathrm{x}_2^E]$ is used to produce the torque commands sent to the robot's actuators. Lower panel: Offline Performance Analysis. Dynamic Protocol: the control performance is assessed by computing Root-mean-square Error (RMSE) and Pearson's Correlation coefficient (r) between the subject's and the robot's joint angles. Isometric Protocol: the control performance is assessed by computing three indices: Completion time ($\mathrm{T_{tot}}$), average speed (V), and Index of Performance (IP).

and DOF 2 EMG data separately, we obtained a four-column subject-specific synergy matrix S

$$S = \left[S_1^F, S_1^E, S_2^F, S_2^E\right]. \tag{3}$$

The EMG signals acquired during the calibration phases were also used to compute the multiplicative factors that were utilized during the online phase to match the relative angular magnitude of motion between the user and the robot (Fig. 3). In particular, for the synergy-based approach, for each DOF separately, given S and the single-DOF EMG data, we computed, by solving a nonnegative least squares constraint problem (Matlab function 'lsqnonneg') the four activation coefficients (A). We then computed y_i as the difference between the two activation coefficients related to the i^{th} DOF

$$\mathrm{y}_i(t) = a_i^E(t) - a_i^F(t). \tag{4}$$

We took the maximum (y_E) and the minimum (y_F) values of y (which corresponded to maximal extension and maximal flexion of the ith DOF, respectively), and we computed $G\_syn_i^E$ and $G\_syn_i^F$ as

$$G\_syn_i^E = \frac{y_E}{\tau_{\mathrm{MAX}}}, \tag{5}$$

$$\text{and} \quad G\_syn_i^F = \frac{y_F}{\tau_{\mathrm{MAX}}} \tag{6}$$

where τ_{MAX} was known *a priori* as the torque that has to be sent to the robot's single-DOF in order to move the DOF from a neutral zero position to the maximal flexion or extension in 2 seconds. The multiplicative factor G_syn_i was then computed as the mean between $G\_syn_i^E$ and $G\_syn_i^F$. Likewise, for the muscle-pair approach, for each DOF separately, given the single-DOF EMG data, we computed z_i as the difference between the two EMG signals that corresponded to the muscles most involved in each of the two directions of articulation of the ith DOF (x^E and x^F)

$$z_i(t) = x_i^F(t) - x_i^E(t). \tag{7}$$

In particular, BIC and TRIC were selected for DOF 1, while AD and PD were used for DOF 2. We took the maximum (z_E) and the minimum (z_F) values of z (which corresponded to maximal extension and maximal flexion of the ith DOF, respectively), and we computed $G\_m\mathrm{Pair}_i^E$ and $G\_m\mathrm{Pair}_i^F$ as

$$G\_m\mathrm{Pair}_i^E = \frac{y_E}{\tau_{\mathrm{MAX}}} \tag{8}$$

$$\text{and} \quad G\_mPair_i^F = \frac{y_F}{\tau_{\mathrm{MAX}}}. \tag{9}$$

As for the synergy-based approach, the multiplicative factor $G\_m\mathrm{Pair}_i$ was then computed as the mean between $G\_m\mathrm{Pair}_i^E$ and $G\_m\mathrm{Pair}_i^F$.

E. Control Analysis

1) Synergy-Based Control: As shown in Fig. 3, the EMG signals acquired in this phase were used for online control of the two DOFs of the robotic arm. In our protocol, we assumed that a system consisting of two biomechanical DOFs (DOF 1 and DOF 2) was driven by four activation signals

$$X(t) = \left[S_1^F, S_1^E, S_2^F, S_2^E\right] \cdot \left[a_1^F(t), a_1^E(t), a_2^F(t), a_2^E(t)\right]^T. \tag{10}$$

Each time instant, given the online nonlinear envelopes of the EMG signals ($X(t)$) and the subject-specific S matrix, the algorithm extracted, by solving a nonnegative least squares constraint problem [32], the four activation signals $(a_1^F, a_1^E, a_2^F, a_2^E)$ that were used for online simultaneous torque-based control of the two DOFs of the robotic arm. In particular, our approach modeled the ith DOF as driven by the difference between the two activation signals related to the DOF, scaled by the multiplicative factor G_syn_i

$$\tau_i(t) = G\_syn_i \cdot \left(a_i^F(t) - a_i^E(t)\right). \tag{11}$$

2) Muscle-Pair Control: As shown in Fig. 3, for each time instant, each DOF of the robotic arm was driven by the difference between the two EMG signals that corresponded to the muscles most involved in each of the two directions of articulation of the DOF (x^F and x^E), scaled by the multiplicative factor $G\_m\mathrm{Pair}_i$

$$\tau_i(t) = G\_m\mathrm{Pair_i} \cdot \left(x_i^F(t) - x_i^E(t)\right). \tag{12}$$

In the Dynamic Protocol, muscle-pair control was an offline simulation run using exactly the same EMG signals recorded during the online synergy-based control phase. On the other hand, since visual feedback was needed for the proper achievement of the Isometric Protocol, muscle-pair control was tested online.

F. Performance Analysis and Statistics

Performance analysis was executed with Matlab R2011b (Mathworks, Natick, MA USA). Statistical analysis was performed using RStudio Version 0.98.981 (RStudio Inc., Boston, MA, USA) and the R-package "lme4" Version 1.1-7 [33]. For the statistics, the significance level was set at 5%.

1) Dynamic Protocol: The subject's and the robot's angular trajectories for DOF 1 and DOF 2 were normalized to their respective ranges, to obtain signals ranging from 0 to 1. The performance of the control algorithm was assessed by computing root-mean-square error (RMSE) and Pearson's Correlation coefficient (r) between the subject's and the robot's joint angles (DOF 1 and DOF 2 separately; see Fig. 3). For this protocol, the purpose of the statistical analysis was twofold. First, it is to compare the synergy-based and the muscle-pair approach. In the second place, the purpose is to test the robustness and the repeatability of the synergies over days. For this reason, we ran a three-way repeated measures ANOVA. For each dependent variable (RMSE and r), the design included three independent within-subject factors, each consisting of two levels (Approach: "Synergy" and "Muscle Pair"; DOF: "DOF 1" and "DOF 2"; Day: "Day 1" and "Day 2"). As a consequence of conveying information from a number of muscles, synergy-based myocontrol is expected to provide control that is more natural and more robust to high co-contraction levels, compared to the traditional muscle-pair approach. This feature is quite important when addressing pathological populations that present aberrant co-contractions of antagonist muscles, as is the case for certain disorders of the control of muscles. To validate our hypothesis, we computed the levels of co-contraction between antagonist pairs of muscles and we investigated a possible correlation with the quality of the performance, in terms of error, for the two control approaches separately. As proposed by Rudolph *et al.* [34], the levels of co-contraction (CC) between BIC and TRIC and between AD and PD were computed as

$$CC = \frac{1}{\text{number of frames}} \sum_{i=1}^{\text{numberoffframes}} \left[\left(\frac{\text{Lower EMG}_i}{\text{Higher EMG}_i} \right) \cdot \left(\text{Lower EMG}_i + \text{Higher EMG}_i\right) \right]. \tag{13}$$

To study the overall correlation between CC and RMSE, we applied a linear mixed effects analysis [35] ("lmer" function in R) because the design of our experiment had multiple measures for each subject. Instead of averaging data for each subject, which implies a loss of information, the use of a linear mixed effect model allowed us to resolve nonindependence by assuming different random intercepts and random slopes for each subject. In particular, for each of the two control approaches, we performed a linear mixed effects analysis on RMSE. As fixed effects, we entered CC (CC of BIC and TRIC for RMSE values obtained from DOF 1; CC of AD and PD for RMSE values obtained from DOF 2) and, as random effects, we had intercepts for subjects, as well as by-subject random slopes for the effect of CC. In order to test if the fixed effect CC significantly affected the dependent variable RMSE, we compared the model including all the factors (Full) against a reduced model without the effect of CC (Null). P-values and Akaike's Information Criterion values (AIC) were obtained by likelihood ratio tests of the Full model with the Null model.

2) Isometric Protocol: The performance of the Isometric Protocol was assessed by computing three indices (Fig. 3). Completion time (T_{tot}) was defined as the time it took the subject to accomplish a successful trial, that is the period between the starting instant and the instant the subject reached the third and last target, minus the resting intervals on each target. The average speed (V) of a successful trial was computed as the ratio between the trajectory length and the time (time-to-target) between two targets, averaged over all three targets. Finally, we computed the Index of Performance (IP), which is defined as the human rate of information processing for a specific control task. In the speed-accuracy model of human movement developed by Fitts [36], the IP for a task of a specified difficulty (ID) is defined as

$$\mathrm{IP} = \frac{\mathrm{ID}}{\text{time to target}} \tag{14}$$

where time-to-target is the time to reach a target of a specified width (W) over a specified distance (d). In this study, to measure the quality of myoelectric control, we use the IP derived from the Shannon formulation of the Fitts' Law [37] extended to 2-D tasks [38], conjecturing that different control approaches will have different rates of information transfer. In particular, to move from one target to another, ID was computed as

$$\mathrm{ID} = \log_2\left(\frac{d}{W} + 1\right) \tag{15}$$

where W is the diameter of the circular target, and d is the angular excursion between the two targets, summed over DOF 1 and DOF 2. To assess the validity of the speed-accuracy tradeoff in the current study, we investigated the linear regression between time-to-target and ID. For each trial, we computed three IP values (one for each target), for a grand total of 18 values per subject (nine for the synergy-based control; nine for the muscle-pair control). The IP value was set to 0 for those targets that were not hit.

Similarly to the Dynamic Protocol, we aimed at investigating possible between-approach and between-day differences in terms of performance. We ran a two-way repeated measures ANOVA for the continuous dependent variables T_{tot}, V, and IP, computed for the successful trials. The design included two independent within-subject factors, each consisting of two levels (Approach: "Synergy" and "Muscle Pair"; Day: "Day 1" and "Day 2").

We investigated a possible correlation with the levels of co-contraction of antagonist muscles and the quality of the performance for the two control approaches in the Isometric Protocol as well. We performed a linear mixed effect analysis on IP. As fixed effects, we entered CC averaged over the two pairs of muscles and, as random effects, we had intercepts for subjects, as well as by-subject random slopes for the effect of CC. To test if the fixed effect CC significantly affected IP, we compared the Full and the reduced Null models through likelihood ratio tests.

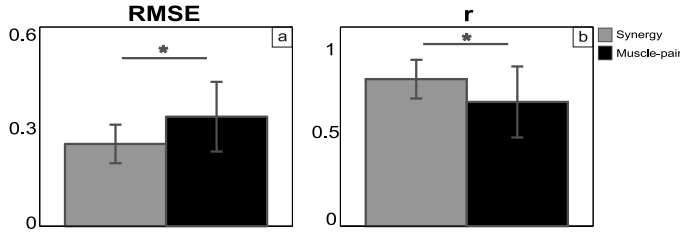

Fig. 4. Results for the Dynamic Protocol. The performances of the two control approaches (synergy-based (gray) and muscle-pair (black)) during dynamic protocol are compared in terms of subject's and robot's angles: a) RMSE and b) correlation coefficient. For each parameter and each control approach, the bars reproduce the mean across subjects and across the 2 DOFs, and the relative standard deviation.

III. Results

Results are reported as mean and standard deviation values.

A. Dynamic Protocol

Three-way repeated measures ANOVA for RMSE between the subject's and the robot's angles reported strong significant effects for within-subject factors Approach ($p = 0.007$) and DOF ($p = 0.021$), with significant interaction between the two factors ($p = 0.022$). In particular, as shown in Fig. 4 panel a, the synergy-based approach showed decreased RMSE values compared to the muscle-pair method (Synergy: 0.248± 0.058; Muscle-pair: 0.330±0.105). The error between the subject's and the robot's angle for DOF 2 was lower than the one for DOF 1 (DOF 1: 0.326± 0.103; DOF 2: 0.253±0.067). The significant interaction shows that the muscle-pair approach leads to increased RMSE values especially for DOF 1. No significant effect emerged for factor Day ($p = 0.870$).

Similar results were reported for the statistics on the linear correlation coefficient r between subject's and robot's angles. Indeed, the statistics reported significant effect for factors Approach ($p = 0.014$) and DOF ($p = 0.003$), with no interaction, while no significance was found for factor Day ($p = 0.978$). The subject's and robot's joint angles showed higher correlation for the synergy-based approach, compared to the muscle-pair approach (Synergy: 0.812± 0.107; Muscle-pair: 0.686± 0.196) (Fig. 4 panel b), and for DOF 2 in comparison with DOF 1 (DOF 1: 0.663± 0.192; DOF 2: 0.835±0.077).

The lowest angular speed of performance, averaged over all subjects, was 0.439 (±0.119) rad/s and 0.468 (±0.065) rad/s for DOF 1 and DOF 2, respectively. The highest was 1.428 (±0.528) rad/s and 0.958 (±0.238) rad/s for DOF 1 and DOF 2, respectively.

As shown in Fig. 5, a significant effect of CC on RMSE was reported for the muscle-pair approach [$\mathrm{AIC_{Full}} = -154.66$; $\mathrm{AIC_{Null}} = -152.45$; $p = 0.040$], with RMSE increasing with CC [Slope for the fixed effect $= 0.56$], while no effect of CC on RMSE emerged for the synergy-based approach [$\mathrm{AIC_{Full}} = -247.42$; $\mathrm{AIC_{Null}} = -249.161$; $p = 0.613$; Slope for the fixed effect $= 0.09$].

B. Isometric Protocol

During the execution of the Isometric Protocol, significant linear regression between time-to-trial and ID was found

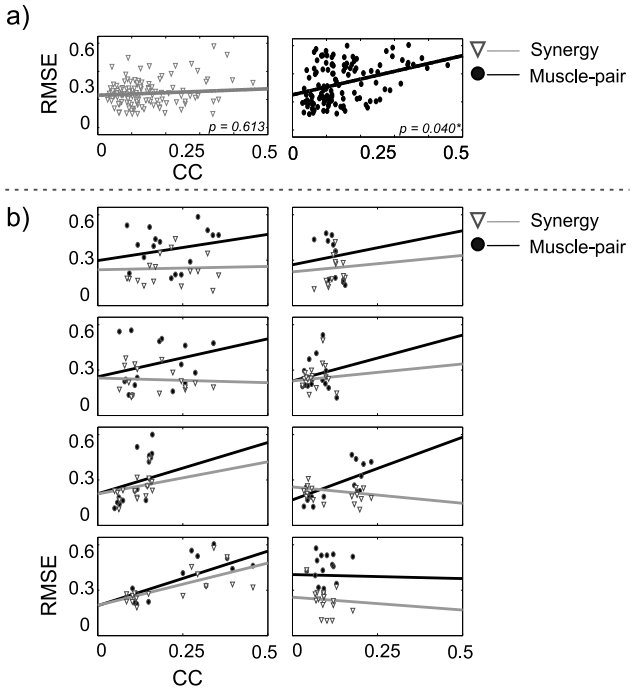

Fig. 5. Correlation between RMSE and co-contraction for the Dynamic Protocol. Panel a: Linear regression between RMSE and co-contraction (CC) for the synergy-based (white triangles) and the muscle-pair approach black circles), computed over all trials of all subjects. Statistics report a significant ($*$) correlation between RMSE and CC for the muscle-pair approach, while no significance was found during the synergy-based control. Panel b: Each subplot represents the linear regression between RMSE and CC for each subject individually. White triangles and black circles show data obtained with the synergy-based and the muscle-pair approaches respectively.

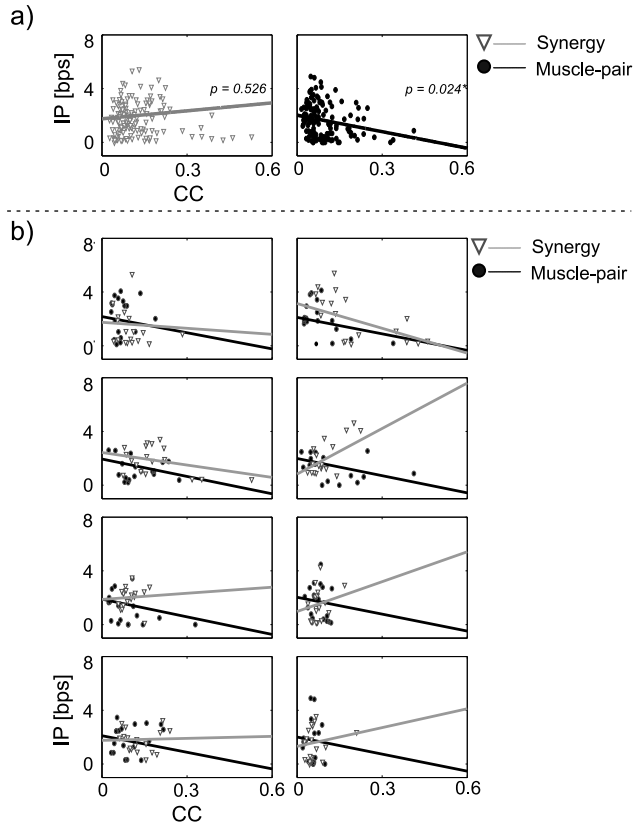

Fig. 6. Correlation between IP and co-contraction for the Isometric Protocol. Panel a: Linear regression between Index of Performance (IP, measured in bit per second [bps]) and co-contraction (CC) for the synergy-based (white triangles) and the muscle-pair approach black circles), computed over all trials of all subjects. Statistics report a significant ($*$) correlation between IP and CC for the muscle-pair approach, while no significance was found during the synergy-based control. Panel b: Each subplot represents the linear regressions between IP and CC for each subject individually. White triangles and black circles show data obtained with the synergy-based and the muscle-pair approaches respectively.

($p = 0.012$). Since the speed-accuracy tradeoff has been widely proposed as an objective measure for real-time performance [39]–[41], this result validates the use of IP, derived from the linear relationship between time and difficulty of the task, to quantify the control performance in the current study.

Two-way ANOVA reported that $\mathrm{T_{tot}}$ was not significantly affected by either Approach or Day ($p = 0.834$ and $p = 0.167$, respectively). Averaged over all participants, the time to accomplish a successful trial was 9.835 ± 4.596 s. Similarly, no significant effect of Approach or Day ($p = 0.447$ and $p = 0.776$, respectively) was found for V. The average speed over all subjects was 15.160 ± 3.687 cm/s. Finally, no difference emerged for IP between the two approaches ($p = 0.907$), or between the two days ($p = 0.586$).

Including all subjects, a higher number of successful trials was accomplished when using the synergy-based control interface, compared to the muscle-pair controller (Synergy: accomplished: 47, failed: 1; Muscle-pair: accomplished: 39; failed: 9).

In addition, for the muscle-pair approach, a significant effect of CC on IP was reported [$\mathrm{AIC_{Full}} = 463.21$; $\mathrm{AIC_{Null}} = 466.29$; $p = 0.024$]. As shown in Fig. 6, IP decreases with increasing CC [Slope for the fixed effect $= -4.20$]. On the other hand, no effect of CC was found on IP for the synergy-based approach [$\mathrm{AIC_{Full}} = 465.64$; $\mathrm{AIC_{Null}} = 464.04$; $p = 0.526$; Slope for the fixed effect $= 1.83$]. This finding suggests that the synergy-based controller may be less affected by abnormal or nonfunctional co-contraction patterns, which characterize a good spectrum of neuromotor disorders.

IV. Discussion

In this study, we tested a semi-supervised approach for synergy-based, online, simultaneous myoelectric control of two DOFs of a robotic arm. The control performance was evaluated in two different conditions: in the first experiment (Dynamic Protocol), the driving signals to control the robot were estimated from muscle activity recorded during the activation of the two DOFs for their full range of motion; while in the second experiment (Isometric Protocol), the subject controlled the myoelectric interface with isometric muscle contractions of the two DOFs.

For both experiments, we compared the performance of the synergy-based approach, with the traditional control scheme based on a pair of independent muscles. We found that, in the Dynamic Protocol, synergy-based online control significantly outperformed the traditional muscle-pair approach in terms of decreased error and increased correlation between the subject's and the robot's joint angles. In the Isometric Protocol, although a higher number of successful trials was accomplished with the synergy-based approach, the quality of the control achieved with the two methods was similar in terms of completion time, average speed, and index of performance. The lack of signif-

icant differences in control quality between the two control schemes may be due to the use of visual feedback during the Isometric Protocol. Indeed, previous studies [24], [42] showed that continuous visual feedback helps subjects to improve online control performance by providing them with the chance to remap the control signals in the proper space in case of inaccuracy of the mapping achieved by the control algorithm. It is therefore likely that the reduced control efficacy for the muscle-pair approach during the Dynamic Protocol was compensated by the availability of visual feedback in the Isometric Protocol. However, since the Dynamic Protocol was not tested in the presence of visual feedback, we are not able to assess how exactly the presence of visual feedback affected the control performance and future work will have to address this open point. The absence of a substantial difference between the two approaches in this second protocol may also be explained by the use of isometric muscle contractions. Indeed, one of the disadvantages of the muscle-pair approach is that, since it records the activity of only a pair of muscles, it is strongly affected if either of the EMG channels is corrupted by noise. We know that the noise components contaminating the EMG signal are enhanced when the signal is obtained during dynamic contractions [43]. Thus, it is likely that myoelectric control mostly benefits from the synergy-based approach, which conveys information from multiple muscles, when the EMG signal is corrupted by a high amount of noise, as for the case of dynamic contractions. Similarly, we can speculate that a myoelectric control approach based on muscle synergies would be particularly suitable when the subject's muscle activity is corrupted by increased sources of variability and co-contraction. Indeed, when extracting synergies from multi-muscle EMG, factorization algorithms such as NMF convert a set of incoming EMG signals into distinguishable and repeatable descriptors, while discarding irrelevant information. As a consequence, muscle synergies are more robust to possible aberrant activity of a single muscle and to abnormal co-contraction levels between pairs of antagonist muscles. This hypothesis is supported by our findings. Indeed, for both protocols, the myoelectric control performance of the muscle-pair approach significantly correlated with the co-contraction levels of antagonist muscles, while no correlation between the quality of the synergy-based controller and the co-contraction levels was reported, suggesting that the performance of the synergy-based approach is more robust to possible nonfunctional co-contraction patterns.

To test the robustness and repeatability of the algorithm, the control performance was evaluated over two days, using the same synergies extracted from the calibration phase on the first day. For both protocols, our results did not report any difference in the control performance between the two days, suggesting that the algorithm was robust to electrode shifts caused by the multiple day experiment, and that the subject-specific synergies extracted from the data recorded during the calibration phase were consistent over days. Although we used a semi-supervised control scheme that only requires a short calibration phase, the myoelectric algorithm was able to provide reliable controllability and online performance without the need for a daily calibration. This is a necessary achievement for clinical and commercial applications.

With the Dynamic Protocol, we showed that the synergy-based control scheme for use in robotic applications is able to provide reliable control signals also when visual feedback is withheld. This finding further validates what was reported by Pistohl and colleagues [29] in the framework of simple cursor control and extends it in the more realistic framework of robotic control, thus supporting the potential of the synergy-based control scheme for successful use in clinical applications. In light of the results reported for the Dynamic Protocol, we are confident that this would also apply to the Isometric Protocol where, because of the design of the current experiment, visual feedback was required to accomplish the task. However, further studies will be needed to test the effect of visual feedback on the control performance of the synergy-based approach when isometric muscle contractions are used.

Future work may also investigate the robustness of the proposed control scheme to possible changes of inertia, for instance by adding weights on the robotic arm

This study recruited naïve subjects who never participated in myocontrol experiments prior to the current one. All of them were able to intuitively and successfully interact with the synergy-based control interface, without the need for significant training and practice.

To validate the different scenarios of the developed control approach, and as a preliminary proof-of-concept, only healthy able-bodied subjects were recruited for the current study. Future work will be needed in order to validate the current algorithm on a vast scenario of different populations, without restricting the current control system to the amputee population, which is typically addressed by research on myoelectric control systems. Myocontrol studies on nonamputee patients are indeed restricted to EMG-controlled robotic exoskeletons and powered orthoses for robot-aided therapy in stroke patients [44], [45]. In particular, to date, no work has focused on patients with severe dyskinetic cerebral palsy (CP) who are unable to achieve effective voluntary movements. Due to early brain injury, these patients are left with a combination of spasticity, dystonia, dyspraxia, and other motor disorders [46]. Commonly available prosthetic devices for patients with severe CP are limited to basic control such as simple computer interfaces for assisted communication or switches for control of an electric wheelchair. Research aimed at developing intuitive and flexible control interface strategies has the potential to provide these patients with significantly improved mobility, manipulation, and functional communication [47], [48]. One of the reasons for using myoelectric control systems with these patients is that, in CP, there is no disconnect between the brain and the spinal cord, so that the EMG signal provides a direct read-out of the movement-related activity in motor cortex. On the other hand, a major obstacle to the use of myoelectric control in patients with CP and arm dystonia is that the EMG signal is corrupted by co-contraction, variability, and increased signal-dependent noise [49]–[52]. Since our findings show that the synergy-based myoelectric controller is robust to the different sources of noise corrupting EMG signals, the proposed control strategy may be a promising tool particularly suitable to help patients with severe dyskinetic CP and other neuromotor disorders that present abnormalities of muscle activity gain functional manipulation, and mobility.

V. Conclusion

To conclude, we successfully validated a semi-supervised approach for synergy-based, online, simultaneous myoelectric control of two DOFs of a robotic arm. All subjects were able to intuitively and easily control the myoelectric interface in different scenarios, using both dynamic and isometric muscle contractions, and without the need for a daily calibration. The proposed control scheme was shown to be robust to co-contraction between antagonist muscles, providing better performance compared to the traditional muscle-pair approach. These properties make the synergy-based control scheme a promising approach for user-friendly control of assistive robotic devices for patients with movement disorders.

Acknowledgment

All authors declare no conflict of interests.

References

[1] R. N. Scott, "Myoelectric control of prostheses and ortheses," *Bull. Prosthet. Res.*, vol. 6, pp. 93–114, 1967.

[2] D. Farina, A. Holobar, R. Merletti, and R. M. Enoka, "Decoding the neural drive to muscles from the surface electromyogram," *Clin. Neurophysiol.*, vol. 121, no. 10, pp. 1616–1623, Oct. 2010.

[3] E. Scheme and K. Englehart, "Electromyogram pattern recognition for control of powered upper-limb prostheses: State of the art and challenges for clinical use," *J. Rehabil. Res. Devel.*, vol. 48, no. 6, p. 643, 2011.

[4] B. Hudgins, P. Parker, and R. N. Scott, "A new strategy for multifunction myoelectric control," *IEEE Trans. Biomed. Eng.*, vol. 40, no. 1, pp. 82–94, Jan. 1993.

[5] K. Englehart and B. Hudgins, "A robust, real-time control scheme for multifunction myoelectric control," *IEEE Trans. Biomed. Eng.*, vol. 50, no. 7, pp. 848–854, Jul. 2003.

[6] N. Jiang, S. Doses, K. R. Müller, and D. Farina, "Myoelectric control of artificial limbs: Is there the need for a change of focus?," *IEEE Signal Process.*, vol. 29, pp. 149–152, Aug. 2012.

[7] A. D. Roche, H. Rehbaum, D. Farina, and O. C. Aszmann, "Prosthetic myoelectric control strategies: A clinical perspective," *Curr. Surg. Rep.*, vol. 2, no. 3, p. 44, Jan. 2014.

[8] D. Atkins, D. C. Y. Heard, and W. H. Donovan, "Epidemiologic overview of individuals with upper-limb loss and their reported research priorities," *J. Prosthet. Orthotics*, vol. 8, no. 1, pp. 2–11, 1996.

[9] A. Pedrocchi, S. Ferrante, E. Ambrosini, M. Gandolla, C. Casellato, T. Schauer, C. Klauer, J. Pascual, C. Vidaurre, M. Gföhler, W. Reichenfelser, J. Karner, S. Micera, A. Crema, F. Molteni, M. Rossini, G. Palumbo, E. Guanziroli, A. Jedlitschka, M. Hack, M. Bulgheroni, E. d'Amico, P. Schenk, S. Zwicker, A. Duschau-Wicke, J. Miseikis, L. Graber, and G. Ferrigno, "MUNDUS project: Multimodal neuroprosthesis for daily upper limb support," *J. Neuroeng. Rehabil.*, vol. 10, p. 66, Jan. 2013.

[10] E. Ambrosini, S. Ferrante, T. Schauer, C. Klauer, M. Gaffuri, G. Ferrigno, and A. Pedrocchi, "A myocontrolled neuroprosthesis integrated with a passive exoskeleton to support upper limb activities," *J. Electromyogr. Kinesiol.*, vol. 24, no. 2, pp. 307–317, Apr. 2014.

[11] M. Ison and P. Artemiadis, "The role of muscle synergies in myoelectric control: Trends and challenges for simultaneous multifunction control," *J. Neural Eng.*, vol. 11, no. 5, Oct. 2014.

[12] B. Popov, "The bio-electrically controlled prosthesis," *J. Bone Joint Surg.*, vol. 47, pp. 421–424, 1965.

[13] A. Bottomley, P. Styles, P. Jilbert, J. Birtill, and J. Truscott, "Prosthetic hand with improved control system for activation by electromyogram signals," U.S. Patent 3,418,662, 1968.

[14] F. Hug, "Can muscle coordination be precisely studied by surface electromyography?," *J. Electromyogr. Kinesiol.*, vol. 21, no. 1, pp. 1–12, Feb. 2011.

[15] J. M. Hahne, F. Biessmann, N. Jiang, H. Rehbaum, D. Farina, F. C. Meinecke, K.-R. Muller, and L. C. Parra, "Linear and non-linear regression techniques for simultaneous and proportional myoelectric control," *IEEE Trans. Neural Syst. Rehabil. Eng.*, vol. 22, no. 2, pp. 269–279, Mar. 2014.

[16] P. K. Artemiadis and K. J. Kyriakopoulos, "EMG-based control of a robot arm using low-dimensional embeddings," *IEEE Trans. Robot.*, vol. 26, no. 2, pp. 393–398, 2009.

[17] D. J. Berger, R. Gentner, T. Edmunds, D. K. Pai, and A. d'Avella, "Differences in adaptation rates after virtual surgeries provide direct evidence for modularity," *J. Neurosci.*, vol. 33, no. 30, pp. 12384–12394, Jul. 2013.

[18] D. J. Berger and A. d'Avella, "Effective force control by muscle synergies," *Front. Comput. Neurosci.*, vol. 8, no. 46, Apr. 2014.

[19] E. Bizzi, V. C. K. Cheung, A. D'Avella, P. Saltiel, and M. Tresch, "Combining modules for movement," *Brain Res. Rev.*, vol. 57, no. 1, pp. 125–133, Jan. 2008.

[20] L. H. Ting and J. L. McKay, "Neuromechanics of muscle synergies for posture and movement," *Curr. Opin. Neurobiol.*, vol. 17, pp. 622–628, 2007.

[21] L. H. Ting and S. A. Chvatal, "Decomposing muscle activity in motor tasks," in *Motor Control, Theories, Experiments and Applications*, F. Danion and M. L. Latash, Eds. New York, NY, USA: Oxford Univ. Press, 2010, pp. 102–138.

[22] M. C. Tresch, V. C. K. Cheung, and A. d'Avella, "Matrix factorization algorithms for the identification of muscle synergies: Evaluation on simulated and experimental data sets," *J. Neurophysiol.*, vol. 95, no. 4, pp. 2199–2212, Apr. 2006.

[23] H. Rehbaum, N. Jiang, L. Paredes, S. Amsuess, B. Graimann, and D. Farina, "Real time simultaneous and proportional control of multiple degrees of freedom from surface EMG: Preliminary results on subjects with limb deficiency," in *Proc. 2012 Annu. Int. Conf. IEEE EMBS*, 2012, pp. 1346–1349.

[24] N. Jiang, I. Vujaklija, H. Rehbaum, B. Graimann, and D. Farina, "Is accurate mapping of EMG signals on kinematics needed for precise online myoelectric control?," *IEEE Trans. Neural Syst. Rehabil. Eng.*, vol. 22, no. 3, pp. 549–558, May 2014.

[25] S. Muceli, N. Jiang, and D. Farina, "Extracting signals robust to electrode number and shift for online simultaneous and proportional myoelectric control by factorization algorithms," *IEEE Trans. Neural Syst. Rehabil. Eng.*, vol. 22, no. 3, pp. 623–633, May 2014.

[26] L. Lee and D. Seung, "Algorithms for non-negative matrix factorization," *Adv. Neural Inf. Process. Syst.*, vol. 13, pp. 556–562, 2001.

[27] S. Muceli and D. Farina, "Simultaneous and proportional estimation of hand kinematics from EMG during mirrored movements at multiple degrees-of-freedom," *IEEE Trans. Neural Syst. Rehabil. Eng.*, vol. 20, no. 3, pp. 371–378, May 2012.

[28] N. Jiang, J. L. Vest-Nielsen, S. Muceli, and D. Farina, "EMG-based simultaneous and proportional estimation of wrist/hand dynamics in uni-lateral trans-radial amputees," *J. Neuroeng. Rehabil.*, vol. 9, no. 1, p. 42, Jun. 2012.

[29] T. Pistohl, C. Cipriani, A. Jackson, and K. Nazarpour, "Abstract and proportional myoelectric control for multi-fingered hand prostheses," *Ann. Biomed. Eng.*, vol. 41, no. 12, pp. 2687–2698, Dec. 2013.

[30] T. D. Sanger, "Bayesian filtering of myoelectric signals," *J. Neurophysiol.*, vol. 97, no. 2, pp. 1839–1845, Feb. 2007.

[31] M. C. Tresch, P. Saltiel, and E. Bizzi, "The construction of movement by the spinal cord," *Nat. Neurosci.*, vol. 2, pp. 162–167, 1999.

[32] L. Charles and R. J. Hanson, *Solving Least Squares Problems*. Upper Saddle River, NJ, USA: Prentice-Hall, 1974.

[33] D. M. Bates, M. Maechler, and B. Bolker, "Lme4: Linear mixed-effects models using S4 classes," *R Package Version 0.999999-0*, 2012.

[34] K. S. Rudolph, M. J. Axe, T. S. Buchanan, J. P. Scholz, and L. Snyder-Mackler, "Dynamic stability in the anterior cruciate ligament deficient knee," *Knee Surg. Sports Traumatol. Arthrosc.*, vol. 9, no. 2, pp. 62–71, 2001.

[35] D. M. Bates, M. Maechler, and B. Bolker, "Lme4: Linear mixed-effects models using S4 classes," *R Package Version 0.999999-0*, 2012.

[36] P. M. Fitts, "The information capacity of the human motor system in controlling the amplitude of movement," *J. Exp. Psychol. Gen.*, vol. 47, pp. 381–391, 1954.

[37] I. S. MacKenzie, "A note on the information-theoretic basis for Fitts' law," *J. Motor Behav.*, vol. 21, pp. 323–330, 1989.

[38] I. S. Mackenzie, W. Buxton, and F. Law, "Extending Fitts' law to two-dimensional tasks," in *Proc. CHI'92 Conf. Human Factors in Computing Systems*, 1992, pp. 219–226.

[39] E. N. Kamavuako, E. J. Scheme, and K. B. Englehart, "Combined surface and intramuscular EMG for improved real-time myoelectric control performance," *Biomed. Signal Process. Contr.*, vol. 10, pp. 102–107, 2014.

[40] E. J. Scheme and K. B. Englehart, "Validation of a selective ensemble-based classification scheme for myoelectric control using a three-dimensional Fitts' law test," *IEEE Trans. Neural Syst. Rehabil. Eng.*, vol. 21, no. 3, pp. 616–623, May 2013.

[41] J. J. Kutch and F. J. Valero-Cuevas, "Challenges and new approaches to proving the existence of muscle synergies of neural origin," *PLoS Comput. Biol.*, vol. 8, p. e1002434, May 2011.
[42] X. Liu and R. A. Scheidt, "Contributions of online visual feedback to the learning and generalization of novel finger coordination patterns," *J. Neurophysiol.*, vol. 99, pp. 2546–2557, 2008.
[43] C. J. de Luca, L. D. Gilmore, M. Kuznetsov, and S. H. Roy, "Filtering the surface EMG signal: Movement artifact and baseline noise contamination," *J. Biomech.*, vol. 43, no. 8, pp. 1573–1579, May 2010.
[44] R. Song, K. Tong, X. Hu, and W. Zhou, "Myoelectrically controlled wrist robot for stroke rehabilitation," *J. Neuroeng. Rehabil.*, vol. 10, no. 1, p. 52, Jan. 2013.
[45] J. Stein, K. Narendran, J. McBean, K. Krebs, and R. Hughes, "Electromyography-controlled exoskeletal upper-limb-powered orthosis for exercise training after stroke," *Am. J. Phys. Med. Rehabil.*, vol. 86, no. 4, Apr. 2007.
[46] T. D. Sanger, "Pediatric movement disorders," *Curr. Opin. Neurol.*, vol. 16, no. 4, pp. 529–535, 2003.
[47] C. Casellato, A. Pedrocchi, G. Zorzi, L. Vernisse, G. Ferrigno, and N. Nardocci, "EMG-based visual-haptic biofeedback: A tool to improve motor control in children with primary dystonia," *IEEE Trans. Neural Syst. Rehabil. Eng.*, vol. 21, no. 3, pp. 474–480, May 2013.
[48] C. Casellato, A. Pedrocchi, G. Zorzi, G. Rizzi, G. Ferrigno, and N. Nardocci, "Error-enhancing robot therapy to induce motor control improvement in childhood onset primary dystonia," *J. Neuroeng. Rehabil.*, vol. 9, no. 46, 2012.
[49] T. D. Sanger, J. Kaiser, and B. Placek, "Reaching movements in childhood dystonia contain signal-dependent noise," *J. Child Neurol.*, vol. 20, no. 6, pp. 489–496, Jun. 2005.
[50] F. Lunardini, M. Bertucco, C. Casellato, N. Bhanpuri, A. Pedrocchi, and T. D. Sanger, "Speed-accuracy trade-off in a trajectory-constrained self-feeding task: A quantitative index of unsuppressed motor noise in children with dystonia," *J. Child Neurol.*, Apr. 2015.
[51] F. Lunardini, S. Maggioni, C. Casellato, M. Bertucco, A. Pedrocchi, and T. D. Sanger, "Increased task-uncorrelated muscle activity in childhood dystonia," *J. Neuroeng. Rehabil.*, Jun. 2015.
[52] C. Casellato, G. Zorzi, A. Pedrocchi, G. Ferrigno, and N. Nardocci, "Reaching and writing movements: Sensitive and reliable tools to measure genetic dystonia in children," *J. Child. Neurol.*, vol. 26, no. 7, Jul. 2011.

Authors' photographs and biographies not available at the time of publication.